Proinflammatory cytokines and cardiovascular damage in chronic hemodialysis patients

Conference Paper *in* Placenta · January 2006

CITATIONS
0

READS
63

7 authors, including:

Luis Michea
University of Chile
98 PUBLICATIONS **2,702** CITATIONS
SEE PROFILE

Paula Ibarra
San Sebastian University
10 PUBLICATIONS **114** CITATIONS
SEE PROFILE

Fernando Figueroa
Universidad de los Andes (Santiago de Chile)
83 PUBLICATIONS **2,497** CITATIONS
SEE PROFILE

Journal of Biotechnology 264 (2017) 29–37

Contents lists available at ScienceDirect

Journal of Biotechnology

journal homepage: www.elsevier.com/locate/jbiotec

Co-synthesis of medium-chain-length polyhydroxyalkanoates and CdS quantum dots nanoparticles in *Pseudomonas putida* KT2440

Barbara Oliva-Arancibia[a], Nicolás Órdenes-Aenishanslins[b], Nicolas Bruna[b], Paula S. Ibarra[a], Flavia C. Zacconi[c], José M. Pérez-Donoso[b], Ignacio Poblete-Castro[a,*]

[a] *Biosystems Engineering Laboratory, Center for Bioinformatics and Integrative Biology (CBIB), Faculty of Biological Sciences, Universidad Andres Bello, República 239, 8370146 Santiago, Chile*

[b] *BioNanotechnology and Microbiology Laboratory, Center for Bioinformatics and Integrative Biology (CBIB), Faculty of Biological Sciences, Universidad Andres Bello, República 239, 8370146 Santiago, Chile*

[c] *Departamento de Química Orgánica, Facultad de Química, Pontificia Universidad Católica de Chile, Vicuña Mackenna 4860, Macul, 78204336 Santiago, Chile*

ARTICLE INFO

Keywords:
MCL-Polyhydroxyalkanoates
CdS quantum dots
Coproduction
Pseudomonas putida

ABSTRACT

Microbial polymers and nanomaterials production is a promising alternative for sustainable bioeconomics. To this end, we used *Pseudomonas putida* KT2440 as a cell factory in batch cultures to coproduce two important nanotechnology materials– medium-chain-length (MCL)-polyhydroxyalkanoates (PHAs) and CdS fluorescent nanoparticles (*i.e.* quantum dots [QDots]). Due to high cadmium resistance, biomass and PHA yields were almost unaffected by coproduction conditions. Fluorescent nanocrystal biosynthesis was possible only in presence of cysteine. Furthermore, this process took place exclusively in the cell, displaying the classical emission spectra of CdS QDots under UV-light exposure. Cell fluorescence, zeta potential values, and particles size of QDots depended on cadmium concentration and exposure time. Using standard PHA-extraction procedures, the biosynthesized QDots remained associated with the biomass, and the resulting PHAs presented no traces of CdS QDots. Transmission electron microscopy located the synthesized PHAs in the cell cytoplasm, whereas CdS nanocrystals were most likely located within the periplasmic space, exhibiting no apparent interaction. This is the first report presenting the microbial coproduction of MCL-PHAs and CdS QDots in *P. putida* KT2440, thus constituting a foundation for further bioprocess developments and strain engineering towards the efficient synthesis of these highly relevant bioproducts for nanotechnology.

1. Introduction

The microbial fermentation of various feedstocks is one of the most sustainable systems for producing chemicals at an industrial scale. This process can yield a wide variety of biochemical compounds, such as polymers, fuels, proteins, amino acids, and, more recently, nanomaterials (Nielsen et al., 2013; Lee and Kim, 2015; Becker et al., 2015; Narayanan and Sakthivel, 2010). Bacterial *Pseudomonas* strains are employed as cell factories for the synthesis of polyhydroxyalkanoates (PHAs) (Poblete-Castro et al., 2014; Prieto et al., 2016). The mechanical and physical properties of PHAs are similar to conventional plastics, thus making this sort of biopolymer one the most promising alternatives for replacing oil-based plastics in the near future (Chen, 2009).

Polyhydroxyalkanoate production is promoted in the cell when the nutritional environment is unbalanced towards high carbon concentrations and the limitation of an inorganic nutrient (*e.g.* O_2, N, or P) (Madison and Huisman, 1999). *Pseudomonas putida* strains, in particular, can naturally produce medium-chain-length-PHAs (MCL-PHAs) from different carbon sources, including glucose, glycerol, fatty acids, and waste materials (Poblete-Castro et al., 2012a). Additionally, *P. putida* is highly versatile metabolically (Santos VAP et al., 2004; Poblete-Castro et al., 2017), a trait that allows this bacterium to cope with adverse growth conditions caused by abiotic factors, including high/low temperatures, elevated pressure, or high metal concentrations (Srivastava et al., 2008; Miller et al., 2009; Follonier et al., 2012). The metal-coping and −conversion abilities of *P. putida* are of particular interest since the wide distribution of heavy metals in the environment, as a result of anthropogenic activities, has risen public and ecological concern due to their high degree of toxicity. Consequently, *Pseudomonas* spp. strains have long been used for bioremediation purposes (Pieper and Reineke, 2000; Wasi et al., 2013). Building on the ability of *Pseudomonas* spp. to diminish metal toxicity in the cell by reducing heavy

Abbreviations: MCL, medium-chain-length; PHA, polyhydroxyalkanoate; QDots, quantum dots

* Corresponding author.
E-mail address: ignacio.poblete@unab.cl (I. Poblete-Castro).

http://dx.doi.org/10.1016/j.jbiotec.2017.10.013
Received 13 March 2017; Received in revised form 17 October 2017; Accepted 18 October 2017
Available online 19 October 2017

metal ions, these bacterial strains have recently been exploited to synthesize cadmium-based quantum dots (QDots) (Gallardo et al., 2014). Fluorescent nanoparticles QDots have a wide array of applications, ranging from optical imagining to drug-delivery platforms (Zrazhevskiy et al., 2010). They have initially been used in biomedicine and biotechnology where target organic molecules are labeled with QDots in order to be tracked and differentiated from other molecules in a complex system like live cells. As they display a broadband absorption spectrum than standard fluorophores, this feature enables them to have a long fluorescent lifetime allowing to separate their signal (unique color) from that of shorter lived species (Michalet et al., 2005). QDots nanoparticles have many applications today, most importantly in displays, lighting, photovoltaic, sensor and life science. Market analysts forecast that the market value of QDots devices and component will be about 4 billion USD by 2020.

The current industrial production of QDots is mostly carried out in nonpolar organic solvents, where the temperature used in the process can modulate the size and shape of the nanocrystals (de Mello Donegá et al., 2006). These processes do not address several environmental aspects such as the use of expensive and toxic organic solvents, which can account for up to 90% of the total production costs, and the high input energy needed within the manufacturing process (Jacob et al., 2016). The microbial production of QDots has opened new avenues for a more sustainable synthesis route compared to chemical production. The bio-based synthesis is more energy efficient, requires a lower input of toxic reagents, and generates nanoparticles with increased biocompatibility and tolerance to harsh conditions (Wegner and Hildebrandt, 2015; Ulloa et al., 2016). They can be purified by using discontinuous sucrose density gradient followed by several centrifugation steps (Park et al., 2016). Furthermore, the size and shape of the resulting nanocrystals can be defined by the culture conditions (*e.g.* pH, reducing agents, and temperature) (Sweeney et al., 2004; Bai et al., 2009). Stable nanoparticles can also be coated with polymers and ligands, thus preventing aggregation, toxic effects, and enzymatic degradation (Pandian et al., 2011). A great deal of attention has recently focused on using biopolymers as matrices for encapsulating fluorescent nanoparticles. This emphasis is due to a growing need to target specific cells under *in vivo* conditions (Hezinger et al., 2008; Tomczak et al., 2013). Biochemical coproduction using microbial strains shows promise as a more cost-competitive option to processes that separately synthesize target compounds (Wang et al., 2012; Hara et al., 2014). The simultaneous production of PHAs and rhamnolipids is possible using the human and plant pathogens *Pseudomonas aeruginosa* and *Thermus thermophilus* HB8 (Pantazaki et al., 2011). Cosynthesis is also possible for polyhydroxybutyrate and 5-aminolevulinic acid in a metabolically engineered *Escherichia coli* strain (Li et al., 2016). Notable, several studies report that bacteria capable of producing PHAs exhibit improved survival and stress tolerances, especially when challenged by oxidative stress (Kadouri et al., 2005). Considering the relevant, increasing need for viable coproduction alternatives of biopolymers, the aim of the present study was to co-synthesize MCL-PHAs and CdS QDots in batch cultures using *P. putida* KT2440 as a cell factory. Focus was given to assessing the effects of cadmium on biomass, PHA yields, and the monomer composition of the biopolymer, as well as to several properties of the synthesized QDots and localization of each compound within the cell.

2. Materials and methods

2.1. Strain and growth conditions

The wild-type *P. putida* KT2440 (DSM 6125, DSMZ, Braunschweig, Germany) was used in this study. Cells were kept as frozen stocks in 25% glycerol at −80 °C. To obtain single colonies, it was plated onto Luria Bertani agar plates after one day incubation at 30 °C. Inoculum was prepared by picking up a single colony from the plate and inoculating it into a 50 mL shake flask containing 10 mL of the defined minimal medium (M9) consisting of 12.8 $g{\cdot}L^{-1}$ $Na_2HPO_4{\cdot}7H_2O$, 3 $g{\cdot}L^{-1}$ KH_2PO4, 0.5 $g{\cdot}L^{-1}$ NH_4Cl, 0.5 $g{\cdot}L^{-1}$ NaCl. This medium was autoclaved and subsequently supplemented with 0.12 $g{\cdot}L^{-1}$ of $MgSO_4{\cdot}7H_2O$, trace elements (6.0 $FeSO_4{\cdot}7H_2O$, 2.7 $CaCO_3$, 2.0 $ZnSO_4{\cdot}H2O$, 1.16 $MnSO_4{\cdot}H_2O$, 0.37 $CoSO_4{\cdot}7H_2O$, 0.33 $CuSO_4{\cdot}5H_2O$, 0.08 H_3BO_3) ($mg{\cdot}L^{-1}$) (filter-sterilized), and 20 mM of decanoate as the unique carbon source. The cells were grown under aerobic conditions at 30 °C in an Ecotron incubator shaker (INFORS HT, Switzerland) set at 160 rpm. By taking a calculated volume of the overnight-grown cell suspension (to begin the PHA-accumulating process with an initial OD_{600} of 0.05), the cells were then inoculated into 500 mL baffled Erlenmeyer flasks with 100 mL of culture medium and cultivated in a rotary shaker as described above.

2.2. Minimal inhibitory concentration (MIC)

MIC-$CdCl_2$ of *P. putida* KT2440 was determined over a wide range of metal concentrations (300–1000 $\mu g{\cdot}mL^{-1}$) in LB liquid and minimal medium supplemented with decanoate 5 mM. Each culture was inoculated with a defined volume of grown cells to achieve an initial OD_{600} value of 0.05 in shaking flask (50 mL). Subsequently cells were grown under aerobic conditions at 30 °C in an Ecotron incubator shaker (INFORS HT, Switzerland) set at 160 rpm for 24 h. The MIC value for cadmium was determined as the value for colony forming units (CFU) showing 99% decrease in bacterial growth when compared with the controls, measured by streaking a series of dilutions of *P. putida* cells onto LB agar plates and incubated in an oven at 30 °C for 24 h.

2.3. Biosynthesis of nanoparticles

180 or 360 ($\mu g{\cdot}mL^{-1}$) of $CdCl_2$ were added to the flask culture at 48 or 68 h of cultivation. To induce the biosynthesis of CdS nanoparticles in *P. putida* KT2440, cysteine was then supplemented to the culture (to a final concentration of 1 mM) at 72 h, samples were collected every hour to evaluate CdS QDots formation *via* fluorescence emission.

2.4. Purification of intracellular nanoparticles

50 mL of culture producing QDots were concentrated by centrifugation at 8000 × *g* for 5 min and washed twice with 50 mM Tris-HCl pH 7.4. Cell lysis was carried out using glass beads (MP-Biomedicals) for 3 cycles of homogenization. The suspension was then further sonicated (10 cycles, 15 s on and 30 s off) to achieve full cell disruption. Subsequently, the resulting solution was centrifuged 10 min at 14,000 x *g* and the supernatant was loaded on a Sephadex column G75 for gel filtration. Subsequently, fluorescent fractions were stored at 4 °C for further characterization.

2.5. Zeta potential analysis of the biosynthesized CdS QDots

The mean superficial charge of the different formulations of nanoparticles was determined by Zeta potential (Zetasizer NanoS90, Malvern Instrument, U.K.). The measurements were carried out at 25 °C using cuvettes DTS1070. To resolve the given values three consecutive measurements were performed (Program Zetasizer version 7.11). In each measure the cuvettes were rinsed with MiliQ grade water and dried. Nanoparticles were diluted 10 times for each measure.

2.6. Size distribution of the purified CdS nanocrystals

The mean size of nanoparticles was determinate for nanoparticle using the tracking acquisition (NTA) method (NanoSight NS300, Malvern Instrument, U.K.). The measurements were carried out at 25 °C and processed with the NanoSight software (NTA 3.2 Dev Build 3.2.16). Between each measurement the plate was rinsed ten times in an equal

volume with MiliQ grade water.

2.7. Quantification of cadmium in the culture broth

50 mL samples of the culture were taken at different time points during the batch culture. Samples were centrifuged at 4000 × *g*, 4 °C for 20 min. The cell pellet was separated from the supernatant, and the liquid fraction stored at −20 °C for further metal analysis. All measurement were conducted using an Inductively Coupled Plasma Mass Spectrometry ICP-MS (ELAN® DRC II PerkinElmer, Norwalk, CT, USA) which used a Meinhard concentric nebulizer, with a flow rate of 1.0 L min-^{1} (Spectron/Glass Expansion, Ventura, CA) connected to a cyclonic spray chamber. A standard 2.0 mm ID quartz injector and a skimmer (0.9 mm orifice diameter) cones were used. Standard, blank, and sample solutions were delivered using a S10 (PerkinElmer) autosampler.

2.8. PHA extraction method

30 mL of culture broth were collected and centrifuged 10 min at 8000 × *g*, and the resulting cell pellet washed twice with 10 mL of NaCl 0.9%. After storage of the sample for 1 day at −20 °C, it was subjected to freeze-drying for 12 h. The dry pellet was then placed in a sealed tube with 5 mL of pure chloroform, and heated at 90 °C for 4 h. Subsequently the PHA-chloroform solution was poured into a vial and exposed to an air stream for 12 h. Both the remaining cell debris and the purified PHA were further exposed to UV-light to evaluate whether the biosynthesized QDots were attached to the biomass or the purified PHA.

2.9. Fluorescence spectroscopy

Fluorescence spectra of purified nanoparticles were determined by using a fluorescent multiplate reader, Synergy H1 M (Biotek Instruments, Inc., Winooski, VY, USA). Fluorescence spectra were obtained after excitation at 370 nm.

2.10. Biomass quantification

Cell growth was evaluated by measuring the OD at 600_{nm} (UV–vis Optizen 3220UV, Korea). The cell dry weight was determined gravimetrically after collection of 10 mL culture broth for 10 min at 4 °C and 9000 × *g* (Eppendorf 5810 R, Hamburg, Germany) in pre-weighed tubes, including a washing step with distilled water, and drying of the obtained pellet at 100 °C until constant weight.

2.11. PHA quantification and characterization

Monomeric composition of PHA, as well as its cellular content, was determined by gas chromatography mass spectrometry (GC/MS) of the methanolyzed polyester. For this purpose, 10 mL culture broth was placed in a falcon tube and centrifuged (10 min, 4 °C, 8000 × *g*), followed by a washing step with distilled water. The supernatant was discarded and the cell pellet was kept at −20 °C for further processing. Methanolysis was then carried out by re-suspending 5–10 mg of lyophilized aliquots in 2 mL chloroform and 2 mL methanol, containing 15% (v·v^{-1}) sulfuric acid and 0.5 mg·mL^{-1} 3-methylbenzoic acid as internal standard, respectively, followed by incubation at 100 °C for 4 h. After cooling to room temperature, 1 mL of demineralized water was added and the organic phase, containing the resulting methyl esters of the PHA monomers, was analyzed by GC-MS. Analysis was performed in a Clarus 680 gas chromatographer coupled with a Clarus SQ 8T mass spectrometer (PerkinElmer Inc., Waltham, Massachusetts, USA). An aliquot (1 µL) of the organic phase was injected into the gas chromatograph at a split ratio of 1:10. Separation of compounds of interest, *i.e.* the methyl esters of 3-hydroxyhexanoate, 3-hydroxyoctanoate, and 3-hydroxydecanoate, was achieved by a FactorFour VF–5 ms capillary column (30 m · 0.25 mm i.d. · 0.25 mm film thickness, Varian Inc., Agilent Technologies). Helium was used as carrier gas at a flow rate of 0.9 mL min^{-1}. Injector and transfer line temperatures were 275 °C and 300 °C, respectively. The oven temperature program was: initial temperature 40 °C for 2 min, then from 40 °C up to 150 °C at a rate of 5 °C min and finally up to 280 °C at a rate of 10 °C min. Positive ions were obtained using electron impact ionization at 70 eV and mass spectra were generated by scanning ions from *m/z* 50 to *m/z* 650. The PHA content (wt%) was defined as the percentage of the cell dry weight (CDW), represented by the polyhydroxyalkanoate.

2.12. Transmission electron microscopy

Bacteria were fixed by chilling the cultures to 4 °C and addition of glutaraldehyde (2%) and formaldehyde (5%). They were then washed with cacodylate buffer (0.01 M cacodylate, 0.01 M $CaCl_2$, 0.01 M $MgCl_2$ 6H2O, 0.09 M sucrose, pH 6.9) and stained with 1% aqueous osmium for 1 h at room temperature. Samples were then dehydrated with a graded series of alcohol (10, 30, 50, 70, 90 and 100%) with incubation for 30 min at each concentration, except for the 70% alcohol, which contained 2% uranyl acetate and was performed overnight. Samples were infiltrated with an epoxy resin, according to the Spurr formula for hard resin, for several days with pure resin. Ultrathin sections were cut with a diamond knife, counterstained with uranyl acetate and lead citrate and examined in a TEM910 transmission electron microscope (Carl Zeiss, Oberkochen, Germany) at an acceleration voltage of 80 kV. Images were taken at calibrated magnifications using a replica. Images were recorded digitally with a Slow-Scan CCD-Camera (ProScan, 1024 × 1024, Scheuring, Germany) with ITEM-Software (Olympus Soft Imaging Solutions, Munster, Germany). Contrast and brightness were adjusted with Adobe Photoshop CS3.

3. Results and discussion

3.1. Co-synthesis of MCL-PHAs and CdS QDots in batch cultures

Bacteria from the *Pseudomonas* genus display different levels of resistance to cadmium concentration depending on the ecological niche they thrive (Lee et al., 2001). While *P. putida* KT2440 can tolerate cadmium stress (Miller et al., 2009; Manara et al., 2012), no data are available for the minimal inhibitory concentration of cadmium in this strain. This value is important since most microbial-based QDots synthesis processes are based on the use of Cd^{2+} salts. Hence, the present study determined the minimal inhibitory concentration for *P. putida* KT2440 in LB liquid and minimal medium supplemented with decanoate as the only carbon source (Table 1). *P. putida* KT2440 presented elevated cadmium resistance (up to 600 µg·mL^{-1}) when cultured in both medium, particularly as compared to *E. coli* (200 µg·mL^{-1}) and other QDots biosynthesizers (Ulloa et al., 2016). PHA-producing conditions were established in batch cultures, with *P. putida* KT2440 cultivated in shake flasks using minimal medium (M9) supplemented with 20 mM decanoate as the only carbon source. After 75 h, approximately 40% of the cell dry weight for *P. putida* KT2440 had accumulated as PHA (Fig. 1**B**). To promote CdS QDots synthesis within the cell, *P. putida* was challenged by high $CdCl_2$ concentrations (*i.e.* 180 and 360 µg·mL^{-1}) at two different time-points during fermentation (*i.e.* 48

Table 1
Cadmium (Cd) minimum inhibitory concentrations for different *Pseudomonas* strains.

Strain	$CdCl_2$ (µg mL^{-1})	Reference
P. putida KT2440	600	This work
Pseudomonas spp. GC05	500	(Gallardo et al., 2014)
P. putida 06909	400	(Lee et al., 2001)
Pseudomonas spp. Pse3	1400	(Plaza et al., 2016)

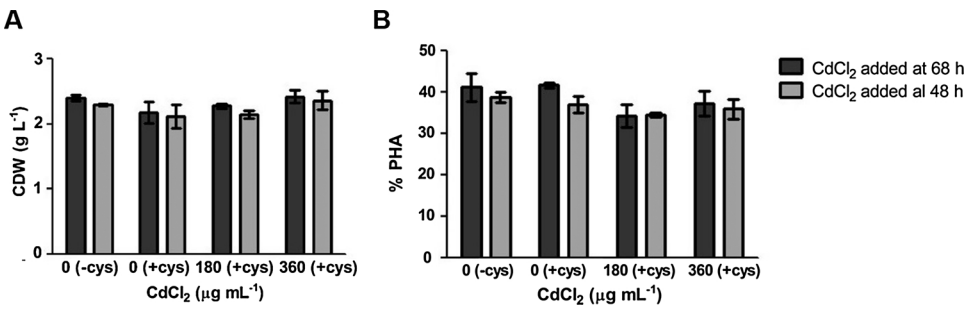

Fig. 1. Biomass and PHA yields on decanoate (20 mM) in *P. putida* KT2440 under different concentrations of **(A)** $CdCl_2$ and **(B)** cysteine. Samples were taken after 75 h of cultivation and represent the mean value of three independent biological replicates.

and 68 h, both in the stationary growth phase). The samples for both challenges were taken at 75 h for PHA and QDots analyses. The aims of this experiment were to evaluate the capacity of *P. putida* KT2440 to cope with high levels of cadmium toxicity and to assess how toxicity impacted cell dry weight and PHA biosynthesis. Remarkably, there were no significant changes in terms of biomass or PHA concentration for any of the tested conditions as compared to cells cultured without $CdCl_2$ (Fig. 1**A**, **B**). Cadmium can damage cells and arrest growth *via* several mechanisms, including the generation of reactive oxygen species (Ferianc and Farewell, 1998), inhibition of DNA replication (Wang and Crowley, 2005), and by damaging the respiratory chain (Pacheco et al., 2008), among others. Growth is fully inhibited in *P. aeruginosa* and *E. coli* strains by 100 $\mu g{\cdot}mL^{-1}$ and 200 $\mu g{\cdot}mL^{-1}$ $CdCl_2$, respectively (Gallardo et al., 2014). In contrast, Plaza et al. (2016) recently showed that *Pseudomonas* strains isolated from Antarctic environments can resist up to 1400 $\mu g{\cdot}mL^{-1}$ $CdCl_2$, in addition to efficiently synthesizing fluorescent CdS QDots on 10 $\mu g{\cdot}mL^{-1}$ $CdCl_2$. Proteomic and transcriptomic studies show that *P. putida* strains exposed to Cd^{2+} activate several genes encoding for enzymes involved in cell-detoxification processes, such as the oxidative stress response, membrane integrity, and efflux pump systems (Miller et al., 2009; Manara et al., 2012). Such features are crucial for a biocatalyzer to efficiently coproduce QDots and PHAs, specifically since one of the process substrates is toxic to the cell and can, therefore, limit the final titer and production using different fermentation modes.

3.2. Characterization of biosynthesized QDots and MCL-PHAs

The microbial synthesis of Cd-based QDots can take place in both inside the cell or in the aqueous extracellular space (Bao et al., 2010; Kominkova et al., 2017). The intracellular sulfide-related compound levels *e.g.* L-cysteine, glutathione, H_2S, have been found to control the synthesis and nucleation of CdS and CdTe fluorescent nanocrystals (Jacob et al., 2016). In addition, there are several studies showing that CdS QDots can be formed chemically in aqueous solution in the presence of H_2S or L-cysteine and a capping agent (Chen and Rosenzweig, 2002; Mo et al., 2012). First, we evaluated whether the medium (M9) used to sustain cell growth or the supernatant of the cell cultures promote the synthesis of CdS nanocrystals. As shown in Fig. 2**A**, there is no fluorescence emission for the different media when supplemented with $CdCl_2$ (with and without L-cysteine) when exposed to UV light, ruling out the possibility of producing CdS nanoparticles without the cells. To promote QDots biosynthesis under PHA-producing conditions in *P. putida* KT2440, the culture was supplemented after 72 h with L-cysteine. Without the addition of this reducing agent, cell pellets showed no change in fluorescence intensity when exposed to UV light (Fig. 2**B**, **C**), indicating that no QDots were synthesized. At high cadmium concentrations (180 or 360 $\mu g{\cdot}mL^{-1}$), bacterial pellets turned highly fluorescent after 74 h of exposure to biosynthesis conditions (Fig. 2**B**, **C**). Cell fluorescence was observed when cadmium was added at 68 or 48 h of cultivation (Fig. 2**B** and **C**, respectively). Fluorescence color slightly differed between times; namely, the addition of cadmium at 48 h of cultivation only generated red fluorescence whereas at 68 h cultivation, yellow and red fluorescent *P. putida* cells were observed depending on the metal concentration. As QDs formation in the cells has been shown to be time-dependent for its appropriate nucleation and increase in size (Sweeney et al., 2004), the addition of cadmium at 68 h accompanied with the induction (cysteine) at 72 h did not give enough time to accomplish this process by the cell, resulting in smaller QDs when 180 $\mu g{\cdot}mL^{-1}$ of cadmium was used. On the other hand, incorporating cadmium at 48 h cultivation, independent of the concentration used in the experiments, might allow the entire nucleation of the metabolized cadmium, giving the same nanocrystals growth (Fig. 2**C**). This result indicates that the emission properties of biosynthesized QDots can be easily managed by adding specific metal concentrations at a define time to *P. putida* cultures. This supposition is supported as growth conditions such as metal concentrations, temperature, pH, and nutrient availability control the size of the obtained QDots (Sweeney et al., 2004; Bai et al., 2009; Pandian et al., 2011). In turn, the particle size of QDots defines emission color after UV irradiation. Smaller QDots emits higher energies than larger QDots, resulting in a shift from blue to red as nanocrystals increase in size (Michalet et al., 2005). Time-dependent changes in the color emission of cell pellets were also monitored to confirm QDots biosynthesis by *P. putida*, as has been previously reported (Monrás et al., 2012; Gallardo et al., 2014; Plaza et al., 2016; Ulloa et al., 2016). This is a particular characteristic of these nanoparticles not observed in other fluorophores such as pigments or biological dyes. As expected, a time-dependent change in emission, moving from green to red fluorescence, was observed in *P. putida* cells exposed to biosynthesis conditions (Fig. 2**D**). As mentioned, *P. putida* KT2440 was able to synthesize QDots only when L-cysteine was added to the medium (Fig. 2). Inspection of the *P. putida* KT2440 genome led to the identification of cysteine desulfhydrase (C-S-lyase, PP_4594), an enzyme that irreversibly coverts cysteine and water into hydrogen sulfide (H_2S), pyruvate, and ammonium. Antioxidant thiols such as cysteine, glutathione, and sulfide are key compounds for QDots formation (Monrás et al., 2012; Mi et al., 2011). Indeed, high intracellular H_2S levels in *Rhodopseudomonas palustri* are directly associated with CdS nanocrystals synthesis *via* C-S-lyase actions (Bai et al., 2009). Antarctic *Pseudomonas sp*. strains also biosynthesize large CdS-QDots quantities together with hydrogen sulfide production, which might serve as the main sulfur donor for nanocrystals synthesis (Gallardo et al., 2014; Plaza et al., 2016).

We also monitored the dynamic of cadmium uptake by *P. putida* KT2440 when the metal salt was added to the culture at 48 and 68 h of cultivation (Fig. 3). The cells rapidly consumed the available cadmium for cultures challenged with 180 $\mu g\ mL^{-1}$, where the Cd^{2+} concentration in the culture broth was under the detection limit ($< 0.01\ \mu g\ mL^{-1}$) after 4 h post addition (Fig. 3**A**). Another scenario was observed for cells exposed at cadmium concentration of 360 $\mu g{\cdot}mL^{-1}$, where approximately 10% of the total cadmium salt remained in the culture broth (Fig. 3**A**). In another set of experiments, $CdCl_2$ was incorporated to the culture at 48 h of cultivation, part of the cadmium accumulated in the cell was secreted (Fig. 3**B**), most likely as a metal detoxification process (Yang et al., 2012), as secretion of the metal from the cells started as soon as L-cysteine was added to the

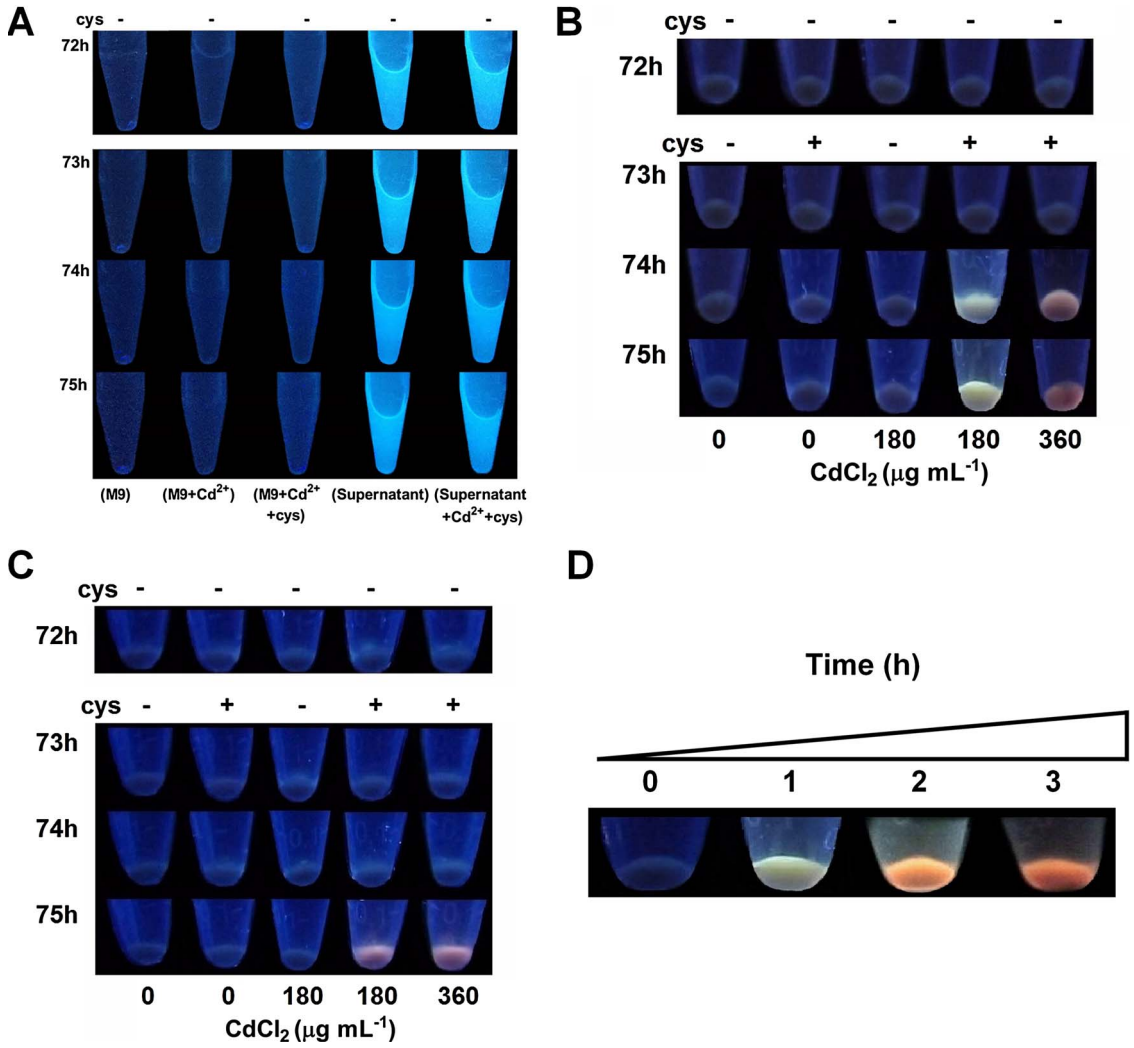

Fig. 2. CdS QDots biosynthesis. *P. putida* KT2440 was grown under various PHA-QDots biosynthesis conditions and the fluorescence when exposed to UV was evaluated every hour. **(A)** Evaluation of the growth medium and supernatant for QDots synthesis **(B)** Cadmium was added at 68 h cultivation. **(C)** Cadmium was added at 48 h cultivation. **(D)** Time-dependent change in the fluorescence color of biosynthesized QDots.

culture broth (denoted by the arrow at 72 h). These experiments are crucial to select an appropriate cadmium concentration to be converted to CdS nanocrystals by the cells, since any remaining cadmium ion in the culture broth turns to be a toxic waste. Taking the values obtained in this study, no more than 300 $\mu g \cdot mL^{-1}$ of $CdCl_2$ should be added to the culture under the set conditions in order to fully convert the used metal to Cd-based QDots.

Following the evaluation of the cadmium removal capacity of KT2440, the obtained QDots were purified and challenged by a strong chelating agent (*i.e.* ethylenediaminetetraacetic acid) to evaluate any possible loss of fluorescence. This acid disrupts the nanostructure by sequestering Cd^{2+} ions from the fluorescent nanocrystal (Durán-Toro et al., 2014). For yellow and red nanoparticles, the addition of ethylenediaminetetraacetic acid provoked a decrease in intensity (Fig. 4), thus confirming that observed fluorescence intensities are associated with a Cd^{2+}-containing nanostructure. To get more insight into the features displayed by the biosynthesized CdS QDots, we exanimated their size as well as their stability based on the zeta potential under

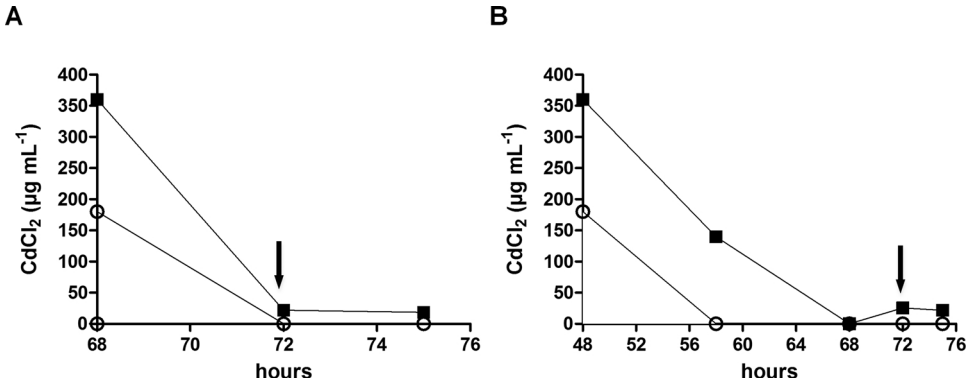

Fig. 3. Dynamic cadmium uptake by *P. putida* KT2440 under PHA-producing conditions. **(A)** $CdCl_2$ was added at 48 h of cultivation. **(B)** $CdCl_2$ was added at 68 h of cultivation. Arrows indicate the addition of cysteine (1 mM) to the cultures. Each experiment was performed by duplicate.

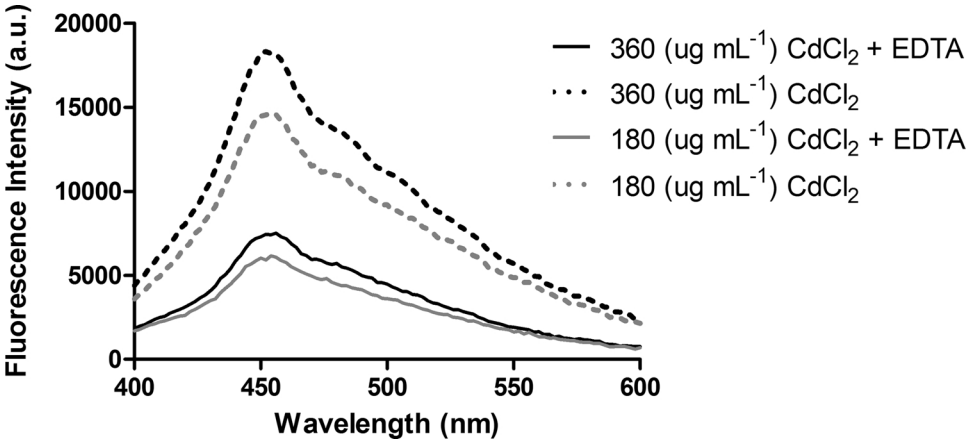

Fig. 4. Effect of ethylenediaminetetraacetic acid (EDTA) on the emission spectra of purified CdS QDots. QDots fluorescent fraction was purified from the cell and challenged to EDTA and the emission spectra recorded (exc. 370 nm).

Table 2
Zeta potential values and particle size determination of the biosynthesized CdS QDs by *P. putida* KT2440 under various conditions.

Condition	Zeta potential (mV)	Particle size (nm)
180 μg mL^{-1} $CdCl_2$ (68 h)	−20.1 ± 6.3	12.5
360 μg mL^{-1} $CdCl_2$ (68 h)	−33.3 ± 9.7	25.4
180 μg mL^{-1} $CdCl_2$ (48 h)	−24.0 ± 5.6	30.6
360 μg mL^{-1} $CdCl_2$ (48 h)	−41.2 ± 6.5	27.5

PHA-producing conditions. All synthesized Cd-based nanocrystals show a zeta potential lower than −20 mV, where the nanocrystals produced with 360 (μg·mL^{-1}) exhibited the highest stability (Table 2). It is worth pointing out that all determined zeta potential values were obtained at pH 6.9. It is well reported that solutions with zeta potential values higher than 30 mV and less than −30 mV are highly stable (Kuznetsova and Rempel, 2015), as they repeal each other avoiding agglomeration (Sankhla et al., 2016), so the nanocrystal produced in this work are very stable in aqueous solution. In terms of particle size distribution, we assessed the purified CdS QDots using a nanoparticle tracking device (NTA, NanoSight®). The QDots particle sizes are shown in Table 2, and as expected, the smallest particle size was found for yellow fluorescent nanoparticles (12.5 nm), while the size of red nanoparticles are in the range of 20–30 nm, where both values are similar to those previously found for these kind of biological-based QDots (Ulloa et al., 2016). In particular, for QDots biosynthesized using 360 μg·mL^{-1} of $CdCl_2$ (added at 48 h of culture), we found a second particle population near 100 nm in the red nanoparticles (S1, D). Ample evidence indicates that "naked" QDots are virtually non-existent in biological systems. Due to a large surface, naked QDots tend to bind various molecules (*e.g.* proteins, lipids, DNA) to reduce surface energy (Mu et al., 2014). Even when CdS nanocrystals have been subjected to various purification procedures, proteins can still be found attached to the biosynthesized QDots (Bai et al., 2009; Mi et al., 2011; Pandian et al., 2011). These amino acids present carbonyl groups with strong binding affinities for metals (Ropo et al., 2016). We believe that this phenomenon might be the main reason explaining the measured size distribution of the biosynthesized nanocrystals in this study. Focus should be given in the future to characterize proteins attached to nanoparticles that exert influence over the size and aggregation of the biosynthesized florescent nanoparticles.

The effect of incorporated cadmium on the monomer composition of the synthesized MCL-PHA was also assessed (Table 3), and no drastic changes were found for any of the tested conditions. As decanoate was used as carbon source, three monomers were identified in the polymeric chain *via* gas-chromatography mass-spectrometry, namely 3-hydroxyhexanoate (C6), 3-hydroxyoctanoate (C8), and 3-hydroxydecanoate (C10). This is in agreement with previous works where *P. putida* strain

Table 3
Monomer composition of medium-chain-length polyhydroxyalkanoates produced by *P. putida* KT2440 batch cultures grown on decanoate.

Condition	Monomer composition (%) C6	C8	C10
0 μg mL^{-1} $CdCl_2$ (−cys)	0.7 ± 0.2	48.9 ± 1.1	50.4 ± 0.8
0 μg mL^{-1} $CdCl_2$ (+cys)	1.3 ± 0.1	53.0 ± 0.7	45.7 ± 0.8
180 μg mL^{-1} $CdCl_2$ (+cys)	1.3 ± 0.3	43.3 ± 0.9	55.4 ± 1.3
360 μg mL^{-1} $CdCl_2$ (+cys)	1.3 ± 0.2	43.9 ± 1.2	54.8 ± 1.5

The data were determined by GC/MS and are given as a relative molar fraction (%) of C6: 3-hydroxyhexanoate, C8: 3-hydroxyoctanoate, C10:3-hydroxydecanoate. $CdCl_2$ was added at 68 h, and samples for analyses were taken after 75 h of cultivation.

produced mcl-PHA using decanoate as the only carbon and energy source (Huijberts et al., 1994; Poblete-Castro et al., 2012b). The addition of Cd^{2+} slightly decreased the molar fraction of C8 (10%). Independent of the cadmium concentration used, C10 was always the main monomer of the resulting monomeric PHA composition (Table 3). Bacterial culture exposure to cadmium can increase the metabolic rates of various cellular pathways, resulting in a shorter lag phase, enhanced specific growth rates, and a reduced total biomass yield (Gibbons et al., 2011). These previously reported bacterial responses could explain the enhanced portion of C10 in the monomeric composition of PHA. Since decanoate must be metabolized at a higher rate when cells are exposed to a high cadmium concentration, more carbon might be funneled for PHA synthesis during the first round of the β-oxidation pathway.

3.3. Standard PHA extraction method separates QDots from MCL-PHAs

Polyhydroxyalkanoates can be isolated from bacterial cells through a number of different extraction methods, such as *via* organic solvents, chemical and enzymatic digestion, mechanical disruption of the cell, and programmable cell lysis systems (Heinrich et al., 2012; Acuña et al., 2017). To evaluate whether the synthesized QDots remain with the cell debris or the purified PHA, a standard chloroform-based extraction method was used (see Materials and methods). The extracted PHAs showed no florescence when exposed to UV light (Fig. 5**A**, **B**). In contrast, the remaining biomass for cells grown in the QDots-producing condition presented a yellowish emission, independent of the cadmium titer used (Fig. 5**C**, **D**). The synthesized QDots remained attached to cell debris after extracting the PHAs with chloroform. Chemical-based QDots are soluble in both water and organic solvents such as chloroform (Yu et al., 2006; Sperling and Parak, 2010). However, biosynthesized QDots are insoluble in chloroform (Plaza et al., 2016), thus explaining why the produced QDots remained with the cell debris.

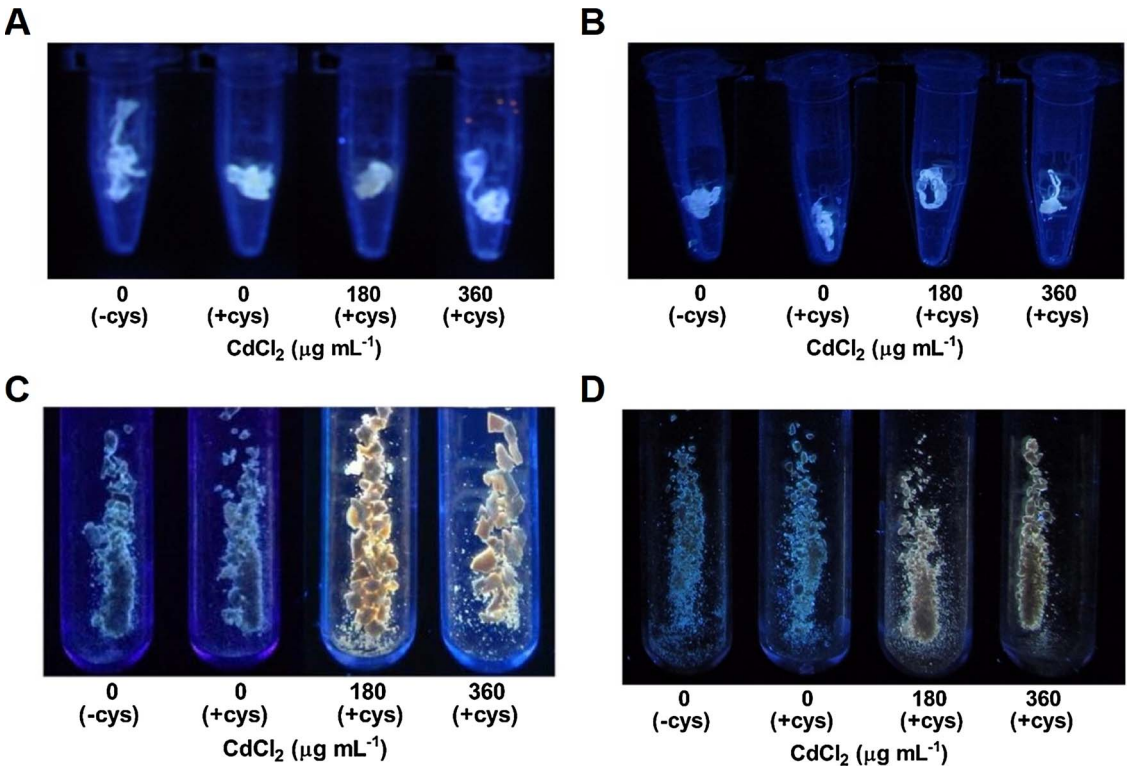

Fig. 5. Purified PHA and cell debris under different cosynthesis conditions using decanoate as the only carbon source. $CdCl_2$ was added at 68 h **(A–C)** or 48 h **(B–D)**.

Indeed, cysteine, glutathione, some enzymes, and a variety of cellular biomolecules can undergo binding during QDots biosynthesis (Monrás et al., 2012; Jacob et al., 2016). Biomolecules attached to the surface of QDots are responsible for the improved properties that characterize most biological QDots, including increased biocompatibility, aqueous solubility, and a tolerance to acidic conditions, among others.

3.4. QDots and PHAs are localized in different sites of the cell

To gain insights into cell morphology, the intracellular localizations of PHAs and CdS QDots were evaluated by transmission electron microscopy (Fig. 6). All micrographs were taken after 75 h of cultivation, when PHAs production was at a maximum. Cells growing under PHA-producing conditions showed irregular inclusion bodies, with granules ranging from one to four units in the cytoplasmic space of the cell (Fig. 6**A**, **D**). In cells challenged by cadmium [360 (μgmL^{-1})] but not induced with cysteine, cell morphology was unchanged, and no metal accumulation was observed (Fig. 6**B**, **E**). Under PHA-QDots co-synthesis conditions, *P. putida* KT2440 appeared to allocate the synthesized CdS QDots as a dense metal layer within the periplasmic space of the cell (Fig. 6**E**, arrows indicate the CdS QDots layer). This feature has been also found in *Pseudomonas stutzeri* when producing AgS nanoparticles (Klaus et al., 1999). In contrast, Antarctic *Pseudomonas spp*. strains accumulate CdS QDots in the cell cytoplasm (Gallardo et al., 2014). It has been proposed that cell walls is the first step in the bioreduction and trapping of the metal ions (Prasad et al., 2016), as well as a nucleation site for nanoparticle synthesis and for further growth into fluorescent nanocrystals (Park et al., 2016). The molecular mechanisms driving the localization of biosynthesized QDots in bacterial cells are still unknown. However, *P. putida* KT2440 possesses several genes encoding for enzymes involved in efflux pump systems that can detoxify cells when challenged with high solvent, antibiotic, and metal concentrations (Godoy et al., 2010). The well-characterized CzcABC metal-extruding pump is responsible for extruding a broad range of heavy metals (Nies, 1999). Therefore, one possible explanation for finding biosynthesized QDots within the periplasm could be the actions of the efflux pump system (Klaus et al., 1999), particularly considering the high concentration of Cd^{2+} used for QDots formation. Once in the periplasmic space, nanoparticles can interact with an organic matrix that contains metal-binding peptides, which creates metal clusters and precipitates (Naik et al., 2002). Another possibility could be that QDots synthesis occurs in the periplasm after Cd^{2+} efflux to this space, namely with the assistance of thiols or reduced enzymes. Periplasmic biomolecules and the oxidative environment present in the periplasm could potentiate CdS seeds formation, which could act as nucleation points for nanocrystal growth (Park et al., 2016). It is worth mentioning that QDots were not found in the supernatants of cell cultures, as supported by a lack of fluorescence detection (Fig. 2**A**). Most of the formed CdS QDots were trapped in the periplasmic cellular space and showed no interaction with the synthesized MCL-PHAs.

4. Conclusions

In this work, we used the versatile bacterium *P. putida* KT2440 to co-synthesize MCL-PHAs and CdS QDots in batch cultures. Given a high cadmium resistance, the biomass and PHA yields were almost unaffected under coproduction conditions. The properties of the biosynthesized CdS QDots nanocrystals depended on culture parameters, with exposure time and metal concentration being key effectors on the QDots emission spectra. Most of the QDots produced by *P. putida* KT2440 were apparently located within the periplasmic space of the cell, but further studies are needed to generate solid evidence supporting this conclusion. In turn, MCL-PHAs were observed in the cytoplasm, with no apparent interactions with the QDots. To our knowledge, this is the first report showing the biological cosynthesis of two important chemicals for nanotechnological applications.

Funding

This work was supported by Fondecyt InicioN°11150174 (to IPC), Fondecyt1151255 (to JMP), INACHRT-25_16 (to JMP), and Nucleo UNABN° DI-816-15/N (to JMP).

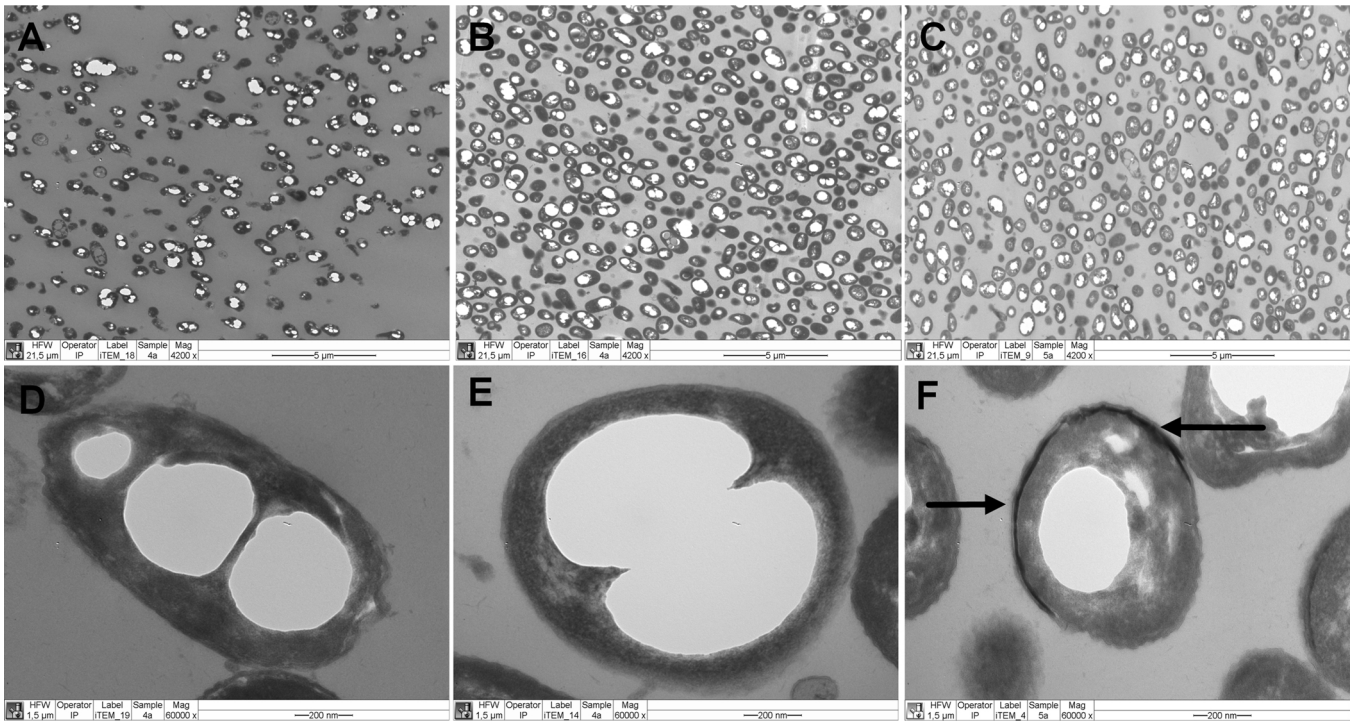

Fig. 6. TEM micrographs of *P. putida* KT2440 cells co-synthesizing PHA and QDots. Cells were grown on 20 mM decanoate and sampled at 75 h. **(A–D)** No $CdCl_2$ nor cysteine was added to the culture. **(B–D)** 360 (μg mL^{-1}) $CdCl_2$ and no cysteine were added to the culture medium. **(C–E)** 360 (μg mL^{-1}) of $CdCl_2$ and cysteine (1 mM) were incorporated to the medium at 68 h of cultivation.

Declaration of interest

The authors declare that there are no conflicts of interest regarding this work.

Contributors

B.O.A., N.O., PI. I., and N. B. performed the experiments. FC.Z carried out the GC–MS analysis. J.M.P. has been involved in the writing of the manuscript. I.P.C. conceived and designed the study as well as analyzed and interpreted the data, and wrote the manuscript. All authors have approved the final article.

Appendix A. Supplementary data

Supplementary data associated with this article can be found, in the online version, at http://dx.doi.org/10.1016/j.jbiotec.2017.10.013.

References

Acuña, J.M.B., Hidalgo-Dumont, C., Pacheco, N., Cabrera, A., Poblete-Castro, I., 2017. A novel programmable lysozyme-based lysis system in Pseudomonas putida for biopolymer production. Sci. Rep. 7, 4373. http://dx.doi.org/10.1038/s41598-017-04741-2.

Bai, H.J., Zhang, Z.M., Guo, Y., Yang, G.E., 2009. Biosynthesis of cadmium sulfide nanoparticles by photosynthetic bacteria Rhodopseudomonas palustris. Colloids Surf. B Biointerfaces 70, 142–146. http://dx.doi.org/10.1016/j.colsurfb.2008.12.025.

Bao, H., Lu, Z., Cui, X., Qiao, Y., Guo, J., Anderson, J.M., Li, C.M., 2010. Extracellular microbial synthesis of biocompatible CdTe quantum dots. Acta Biomater. 6, 3534–3541. http://dx.doi.org/10.1016/j.actbio.2010.03.030.

Becker, J., Lange, A., Fabarius, J., Wittmann, C., 2015. Top value platform chemicals: bio-based production of organic acids. Curr. Opin. Biotechnol. 36, 168–175. http://dx.doi.org/10.1016/j.copbio.2015.08.022.

Chen, Y., Rosenzweig, Z., 2002. Luminescent CdS quantum dots as selective ion probes. Anal. Chem. 74, 5132–5138. http://dx.doi.org/10.1021/ac0258251.

Chen, G.-Q., 2009. A microbial polyhydroxyalkanoates (PHA) based bio- and materials industry. Chem. Soc. Rev. 38, 2434–2446. http://dx.doi.org/10.1039/B812677C.

de Mello Donegá, C., Bode, M., Meijerink, A., 2006. Size- and temperature-dependence of exciton lifetimes in CdSe quantum dots. Phys. Rev. B 74, 85320.

Durán-Toro, V., Gran-Scheuch, A., Órdenes-Aenishanslins, N., Monrás, J.P., Saona, L.A., Venegas, F.A., Chasteen, T.G., Bravo, D., Pérez-Donoso, J.M., 2014. Quantum dot-based assay for Cu2+ quantification in bacterial cell culture. Anal. Biochem. 450, 30–36. http://dx.doi.org/10.1016/j.ab.2014.01.001.

Ferianc, P., Farewell, A., 1998. The cadmium-stress stimulon of Escherichia coli K-12. Microbiology 144, 1045–1050.

Follonier, S., Henes, B., Panke, S., Zinn, M., 2012. Putting cells under pressure: a simple and efficient way to enhance the productivity of medium-chain-length polyhydroxyalkanoate in processes with Pseudomonas putida KT2440. Biotechnol. Bioeng. 109, 451–461. http://dx.doi.org/10.1002/bit.23312.

Gallardo, C., Monrás, J.P., Plaza, D.O., Collao, B., Saona, L.A., Durán-Toro, V., Venegas, F.A., Soto, C., Ulloa, G., Vásquez, C.C., Bravo, D., Pérez-Donoso, J.M., 2014. Low-temperature biosynthesis of fluorescent semiconductor nanoparticles (CdS) by oxidative stress resistant Antarctic bacteria. J. Biotechnol. 187, 108–115. http://dx.doi.org/10.1016/j.jbiotec.2014.07.017.

Gibbons, S.M., Feris, K., McGuirl, M.A., Morales, S.E., Hynninen, A., Ramsey, P.W., Gannon, J.E., 2011. Use of microcalorimetry to determine the costs and benefits to pseudomonas putida strain KT2440 of harboring cadmium efflux genes. Appl. Environ. Microbiol. 77, 108–113.

Godoy, P., Molina-Henares, A.J., De La Torre, J., Duque, E., Ramos, J.L., 2010. Characterization of the RND family of multidrug efflux pumps: in silico to in vivo confirmation of four functionally distinct subgroups. Microb. Biotechnol. 3, 691–700. http://dx.doi.org/10.1111/j.1751-7915.2010.00189.x.

Hara, K.Y., Araki, M., Okai, N., Wakai, S., Hasunuma, T., Kondo, A., 2014. Development of bio-based fine chemical production through synthetic bioengineering. Microb. Cell Fact. 13, 173. http://dx.doi.org/10.1186/s12934-014-0173-5.

Heinrich, D., Madkour, M.H., Al-Ghamdi, M.A., Shabbaj, I.I., Steinbüchel, A., 2012. Large scale extraction of poly(3-hydroxybutyrate) from Ralstonia eutropha H16 using sodium hypochlorite. AMB Express 2, 59. http://dx.doi.org/10.1186/2191-0855-2-59.

Hezinger, A.F.E., Teßmar, J., Göpferich, A., 2008. Polymer coating of quantum dots – a powerful tool toward diagnostics and sensorics. Eur. J. Pharm. Biopharm. 68, 138–152. http://dx.doi.org/10.1016/j.ejpb.2007.05.013.

Huijberts, G.N., de Rijk, T.C., de Waard, P., Eggink, G., 1994. 13C nuclear magnetic resonance studies of Pseudomonas putida fatty acid metabolic routes involved in poly (3-hydroxyalkanoate) synthesis. J. Bacteriol. 176, 1661–1666.

Jacob, J.M., Lens, P.N.L., Balakrishnan, R.M., 2016. Microbial synthesis of chalcogenide semiconductor nanoparticles: a review. Microb. Biotechnol. 9, 11–21. http://dx.doi.org/10.1111/1751-7915.12297.

Kadouri, D., Jurkevitch, E., Okon, Y., Castro-Sowinski, S., 2005. Ecological and agricultural significance of bacterial polyhydroxyalkanoates. Crit. Rev. Microbiol. 31, 55–67. http://dx.doi.org/10.1080/10408410590899228.

Klaus, T., Joerger, R., Olsson, E., Granqvist, C.-G., 1999. Silver-based crystalline nanoparticles, microbially fabricated. Proc. Natl. Acad. Sci. 96, 13611–13614.

Kominkova, M., Milosavljevic, V., Vitek, P., Polanska, H., Cihalova, K., Dostalova, S., Hynstova, V., Guran, R., Kopel, P., Richtera, L., Masarik, M., Brtnicky, M., Kynicky, J., Zitka, O., Adam, V., 2017. Comparative study on toxicity of extracellularly biosynthesized and laboratory synthesized CdTe quantum dots. J. Biotechnol. 241, 193–200. http://dx.doi.org/10.1016/j.jbiotec.2016.10.024.

Kuznetsova V, Y., Rempel, A.A., 2015. Size and zeta potential of CdS nanoparticles in stable aqueous solution of EDTA and NaCl. Inorg. Mater. 51, 215–219. http://dx.doi.org/10.1134/S0020168515020119.
Lee, S.Y., Kim, H.U., 2015. Systems strategies for developing industrial microbial strains. Nat. Biotechnol. 33, 1061–1072.
Lee, S.-W., Glickmann, E., Cooksey, D.A., 2001. Chromosomal locus for cadmium resistance in Pseudomonas putida consisting of a cadmium-transporting ATPase and a MerR family response regulator. Appl. Environ. Microbiol. 67, 1437–1444.
Li, T., Guo, Y.-Y., Qiao, G.-Q., Chen, G.-Q., 2016. Microbial synthesis of 5-aminolevulinic acid and its coproduction with polyhydroxybutyrate. ACS Synth. Biol. 5, 1264–1274. http://dx.doi.org/10.1021/acssynbio.6b00105.
Madison, L.L., Huisman, G.W., 1999. Metabolic engineering of poly(3-hydroxyalkanoates): from DNA to plastic. Microbiol. Mol. Biol. Rev. 63, 21–53.
Manara, A., DalCorso, G., Baliardini, C., Farinati, S., Cecconi, D., Furini, A., 2012. Pseudomonas putida response to cadmium: changes in membrane and cytosolic proteomes. J. Proteome Res. 11, 4169–4179. http://dx.doi.org/10.1021/pr300281f.
Mi, C., Wang, Y., Zhang, J., Huang, H., Xu, L., Wang, S., Fang, X., Fang, J., Mao, C., Xu, S., 2011. Biosynthesis and characterization of CdS quantum dots in genetically engineered Escherichia coli. J. Biotechnol. 153, 125–132. http://dx.doi.org/10.1016/j.jbiotec.2011.03.014.
Michalet, X., Pinaud, F.F., Bentolila, L.A., Tsay, J.M., Doose, S., Li, J.J., Sundaresan, G., Wu, A.M., Gambhir, S.S., Weiss, S., 2005. Quantum dots for live cells, in vivo imaging, and diagnostics. Science 307, 538–544. http://dx.doi.org/10.1126/science.1104274.
Miller, C.D., Pettee, B., Zhang, C., Pabst, M., McLean, J.E., Anderson, A.J., 2009. Copper and cadmium: responses in Pseudomonas putida KT2440. Lett. Appl. Microbiol. 49, 775–783. http://dx.doi.org/10.1111/j.1472-765X.2009.02741.x.
Mo, Y., Tang, Y., Gao, F., Yang, J., Zhang*, Y., 2012. Synthesis of fluorescent CdS quantum dots of tunable light emission with a new in situ produced capping agent. Ind. Eng. Chem. Res. 51, 5995–6000. http://dx.doi.org/10.1021/ie201826e.
Monrás, J.P., Díaz, V., Bravo, D., Montes, R.A., Chasteen, T.G., Osorio-Román, I.O., Vásquez, C.C., Pérez-Donoso, J.M., 2012. Enhanced glutathione content allows the in vivo synthesis of fluorescent CdTe nanoparticles by Escherichia coli. PLoS One 7, e48657.
Mu, Q., Jiang, G., Chen, L., Zhou, H., Fourches, D., Tropsha, A., Yan, B., 2014. Chemical basis of interactions between engineered nanoparticles and biological systems. Chem. Rev. 114, 7740–7781. http://dx.doi.org/10.1021/cr400295a.
Naik, R.R., Stringer, S.J., Agarwal, G., Jones, S.E., Stone, M.O., 2002. Biomimetic synthesis and patterning of silver nanoparticles. Nat. Mater. 1, 169–172.
Narayanan, K.B., Sakthivel, N., 2010. Biological synthesis of metal nanoparticles by microbes. Adv. Colloid Interface Sci. 156, 1–13. http://dx.doi.org/10.1016/j.cis.2010.02.001.
Nielsen, J., Larsson, C., van Maris, A., Pronk, J., 2013. Metabolic engineering of yeast for production of fuels and chemicals. Curr. Opin. Biotechnol. 24, 398–404. http://dx.doi.org/10.1016/j.copbio.2013.03.023.
Nies, D.H., 1999. Microbial heavy-metal resistance. Appl. Microbiol. Biotechnol. 51, 730–750. http://dx.doi.org/10.1007/s002530051457.
Pacheco, C.C., Passos, J.F., Castro, A.R., Moradas-Ferreira, P., De Marco, P., 2008. Role of respiration and glutathione in cadmium-induced oxidative stress in Escherichia coli K-12. Arch. Microbiol. 189, 271–278. http://dx.doi.org/10.1007/s00203-007-0316-8.
Pandian, S.R.K., Deepak, V., Kalishwaralal, K., Gurunathan, S., 2011. Biologically synthesized fluorescent CdS NPs encapsulated by PHB. Enzyme Microb. Technol. 48, 319–325. http://dx.doi.org/10.1016/j.enzmictec.2011.01.005.
Pantazaki, A.A., Papaneophytou, C.P., Lambropoulou, D.A., 2011. Simultaneous polyhydroxyalkanoates and rhamnolipids production by Thermus thermophilus HB8. AMB Express 1, 17. http://dx.doi.org/10.1186/2191-0855-1-17.
Park, T.J., Lee, K.G., Lee, S.Y., 2016. Advances in microbial biosynthesis of metal nanoparticles. Appl. Microbiol. Biotechnol. 100, 521–534. http://dx.doi.org/10.1007/s00253-015-6904-7.
Pieper, D.H., Reineke, W., 2000. Engineering bacteria for bioremediation. Curr. Opin. Biotechnol. 11, 262–270. http://dx.doi.org/10.1016/S0958-1669(00)00094-X.
Plaza, D.O., Gallardo, C., Straub, Y.D., Bravo, D., Pérez-Donoso, J.M., 2016. Biological synthesis of fluorescent nanoparticles by cadmium and tellurite resistant Antarctic bacteria: exploring novel natural nanofactories. Microb. Cell Fact. 15, 76. http://dx.doi.org/10.1186/s12934-016-0477-8.
Poblete-Castro, I., Becker, J., Dohnt, K., dos Santos, V.M., Wittmann, C., 2012a. Industrial biotechnology of Pseudomonas putida and related species. Appl. Microbiol. Biotechnol. 93, 2279–2290. http://dx.doi.org/10.1007/s00253-012-3928-0.
Poblete-Castro, I., Escapa, I.F., Jager, C., Puchalka, J., Chi Lam, C., Schomburg, D., Prieto, M.A., Martins dos Santos, V., 2012b. The metabolic response of P. putida KT2442 producing high levels of polyhydroxyalkanoate under single- and multiple-nutrient-limited growth: highlights from a multi-level omics approach. Microb. Cell Fact. 11, 34.
Poblete-Castro, I., Binger, D., Oehlert, R., Rohde, M., 2014. Comparison of mcl-Poly(3-hydroxyalkanoates) synthesis by different Pseudomonas putida strains from crude glycerol: citrate accumulates at high titer under PHA-producing conditions. BMC Biotechnol. 14, 962.
Poblete-Castro, I., Borrero-de Acuña, J.M., Nikel, P.I., Kohlstedt, M., Wittmann, C., 2017. Host organism: pseudomonas putida. Industrial Biotechnology. Wiley-VCH, pp. 299–326.
Prasad, R., Pandey, R., Barman, I., 2016. Engineering tailored nanoparticles with microbes: quo vadis? Wiley Interdiscip. Rev. Nanomed. Nanobiotechnol. 8, 316–330. http://dx.doi.org/10.1002/wnan.1363.
Prieto, A., Escapa, I.F., Martínez, V., Dinjaski, N., Herencias, C., de la Peña, F., Tarazona, N., Revelles, O., 2016. A holistic view of polyhydroxyalkanoate metabolism in Pseudomonas putida. Environ. Microbiol. 18, 341–357.
Ropo, M., Blum, V., Baldauf, C., 2016. Trends for isolated amino acids and dipeptides: conformation, divalent ion binding, and remarkable similarity of binding to calcium and lead. Sci. Rep. 6, 35772.
Sankhla, A., Sharma, R., Yadav, R.S., Kashyap, D., Kothari, S.L., Kachhwaha, S., 2016. Biosynthesis and characterization of cadmium sulfide nanoparticles – an emphasis of zeta potential behavior due to capping. Mater. Chem. Phys. 170, 44–51. http://dx.doi.org/10.1016/j.matchemphys.2015.12.017.
Santos VAP, M., d Heim, S., Stratz, M., Timmis, K.N., 2004. Insights into the genomic basis of niche specificity of Pseudomonas putida strain KT2440. Env. Microbiol. 6, 1264–1286.
Sperling, R.A., Parak, W.J., 2010. Surface modification, functionalization and bioconjugation of colloidal inorganic nanoparticles. Philos. Trans. R. Soc. A Math. Phys. Eng. Sci. 368 (133), LP–1383.
Srivastava, S., Yadav, A., Seem, K., Mishra, S., Chaudhary, V., Nautiyal, C.S., 2008. Effect of high temperature on pseudomonas putida NBRI0987 biofilm formation and expression of stress sigma factor RpoS. Curr. Microbiol. 56, 453–457. http://dx.doi.org/10.1007/s00284-008-9105-0.
Sweeney, R.Y., Mao, C., Gao, X., Burt, J.L., Belcher, A.M., Georgiou, G., Iverson, B.L., 2004. Bacterial biosynthesis of cadmium sulfide nanocrystals. Chem. Biol. 11, 1553–1559. http://dx.doi.org/10.1016/j.chembiol.2004.08.022.
Tomczak, N., Liu, R., Vancso, J.G., 2013. Polymer-coated quantum dots. Nanoscale 5, 12018–12032. http://dx.doi.org/10.1039/C3NR03949H.
Ulloa, G., Collao, B., Araneda, M., Escobar, B., Álvarez, S., Bravo, D., Pérez-Donoso, J.M., 2016. Use of acidophilic bacteria of the genus Acidithiobacillus to biosynthesize CdS fluorescent nanoparticles (quantum dots) with high tolerance to acidic pH. Enzyme Microb. Technol. 95, 217–224. http://dx.doi.org/10.1016/j.enzmictec.2016.09.005.
Wang, A., Crowley, D.E., 2005. Global gene expression responses to cadmium toxicity in Escherichia coli. J. Bacteriol. 187, 3259–3266. http://dx.doi.org/10.1128/JB.187.9.3259-3266.2005.
Wang, Y., Wang, D., Wei, G., Shao, N., 2012. Enhanced co-production of S-adenosylmethionine and glutathione by an ATP-oriented amino acid addition strategy. Bioresour. Technol. 107, 19–24. http://dx.doi.org/10.1016/j.biortech.2011.12.030.
Wasi, S., Tabrez, S., Ahmad, M., 2013. Use of Pseudomonas spp. for the bioremediation of environmental pollutants: a review. Environ. Monit. Assess. 185, 8147–8155. http://dx.doi.org/10.1007/s10661-013-3163-x.
Wegner, K.D., Hildebrandt, N., 2015. Quantum dots: bright and versatile in vitro and in vivo fluorescence imaging biosensors. Chem. Soc. Rev. 44, 4792–4834. http://dx.doi.org/10.1039/C4CS00532E.
Yang, Y., Mathieu, J.M., Chattopadhyay, S., Miller, J.T., Wu, T., Shibata, T., Guo, W., Alvarez, P.J.J., 2012. Defense mechanisms of Pseudomonas aeruginosa PAO1 against quantum dots and their released heavy metals. ACS Nano 6, 6091–6098. http://dx.doi.org/10.1021/nn3011619.
Yu, G., Liang, J., He, Z., Sun, M., 2006. Quantum dot-mediated detection of γ-aminobutyric acid binding sites on the surface of living pollen protoplasts in tobacco. Chem. Biol. 13, 723–731. http://dx.doi.org/10.1016/j.chembiol.2006.05.007.
Zrazhevskiy, P., Sena, M., Gao, X., 2010. Designing multifunctional quantum dots for bioimaging, detection, and drug delivery. Chem. Soc. Rev. 39, 4326–4354. http://dx.doi.org/10.1039/b915139g.